

On Sliding Mode Control for Three-phase Voltage Source Converters

Weipeng Yang, *Member, IAENG*, Aimin Zhang, Jungang Li, Jianhua Wang and Hang Zhang

Abstract—For three-phase voltage source converters (VSC), current control in d - q reference frame (RF) and direct power control (DPC) under balanced voltage conditions (BVC) are regulation problems, and current control in the α - β RF (CCAB) is a tracking problem. Conventional sliding mode control-based proportional controllers are sometimes adopted for current and power regulation, proportional plus resonant controllers are often used for CCAB. However, these controllers cannot ensure accurate current and power control due to time delays in the control loops. In this paper, practical SMC-based regulation and tracking controllers for VSC are designed. For current and power regulation, an integral SMC controller of which integral actions are included in both the control law and the sliding manifold is proposed. For CCAB, a current tracking controller, including proportional, resonant and derivative control laws is presented. System stability in Lyapunov sense is guaranteed and convergence of the state errors to zero is strictly proved based on Barbalat' Lemma. Finally, simulation studies on DPC under BVC and on CCAB are conducted to verify the effectiveness and to demonstrate superiority of the proposed controllers.

Index Terms—Voltage source converter, sliding mode control, current control, direct power control, tracking control

I. INTRODUCTION

IN recent years, application of three-phase voltage source converter (VSC) has been increasing rapidly in different industrial sectors, owing to advantages such as flexible power control, high power quality, minimization of filters, etc [1-5]. However, the operating conditions of electric power system change frequently and violently; parameter uncertainty and various kinds of disturbance are common. Thus, a control system that provides high performance and strong robustness of the VSC is of great importance.

Current control and direct power control (DPC) are the two most frequently adopted strategies for VSC [6-7]. Based on characteristics of the controlled variables, current control and

DPC can be classified into regulation and tracking problems. Current control in d - q reference frame (RF) and DPC under balanced voltage conditions (BVC) are regulation problems, and current control in the static two-phase (α - β) RF (CCAB) is a tracking problem.

Regarding current and power regulation for VSC, sliding mode control (SMC)-based strategies are studied extensively to improve system robustness. In [8], a SMC-based current control strategy for high voltage direct current (VSC-HVDC) system is proposed. In [9], a SMC-based DPC strategy for grid-connected inverter (GCI) under both balanced and unbalanced grid voltage conditions is proposed. In [10,11], DPC strategies using SMC approach for doubly fed induction generator (DFIG) under unbalanced grid voltage conditions are presented. However, in the previous current control and DPC strategies, as the current and power dynamics have a relative degree of one, the (d - and q -axis) current errors and (active and reactive) power errors are used as corresponding sliding manifolds (SM), following the conventional SMC (CSMC) design process. Consequently, the designed current and power controllers are in essence SMC-based proportional controllers.

SMC-based DPC strategies for GCI and DFIG system with integral SM are proposed in [12] and [13,14], respectively. However, integral actions are contained only in the switching functions. The controllers are still equivalent to proportional controllers from control force's point of view. In fact, as large time delays exist in the control loops, current or power control errors can be reduced to some extent but cannot be fully eliminated by the CSMC-based proportional controllers. The authors of [15] discovered this point in CSMC-based control for dc-dc converters and revealed steady state errors increase with the decrease of switching frequency. However, double integral SM is used to remedy this deficiency. In [16-17], this problem is solved through inclusion of integral actions in the control laws and the SMs. However, working principle and features of the designed controllers are not analyzed.

Regarding CCAB, as the currents in α - β RF are sinusoidal signals, proportional plus resonant (PR) controllers are often adopted aiming at achieving accurate current control. In [18], PR-based current control for VSC-HVDC system is presented. In [19,20], PR-based current control for modular multi-level converter HVDC system is presented. In the PR controllers, function of the resonant control law is to provide infinite gain at the resonant frequency, and thus steady state errors can be eliminated at this interested frequency. However, due to large time delays exist in the control loops, accurate current control cannot be achieved simply with PR controllers, and moreover,

Manuscript received June 03, 2017; revised February 03, 2018. This work was supported in part by the National Key Research and Development Program of China (2016YFB0900500).

Weipeng Yang is with the State Key Laboratory of Electrical Insulation and Power Equipment and School of Electrical Engineering, Xi'an Jiaotong University, Xi'an 710049, PRC (e-mail: wpyang@stu.xjtu.edu.cn).

Aimin Zhang (Corresponding Author) is with the School of Electronic and Information Engineering, Xi'an Jiaotong University, Xi'an, 710049, PRC (phone: +86-29-8266-8665-167; e-mail: zhangam@mail.xjtu.edu.cn).

Jungang Li is with the State Grid Xuji Group Corporation, Xu Chang, 461000, PRC (e-mail: aogusdu@gmail.com).

Jianhua Wang is with the State Key Laboratory of Electrical Insulation and Power Equipment and School of Electrical Engineering, Xi'an Jiaotong University, Xi'an 710049, PRC (e-mail: jhwang_xjtu@163.com).

Hang Zhang is with the School of Electrical Engineering, Xi'an Jiaotong University, Xi'an 710049, PRC (e-mail: zhangh@mail.xjtu.edu.cn).

system robustness is not guaranteed. In [21], a reduced order integrator is presented for GCI to control power errors under unbalanced grid voltage conditions. However, this method is complex and system robustness is not addressed.

In this paper, practical SMC-based regulation and tracking controllers for VSC are designed. For current and power regulation, an integral SMC (ISMC) controller with integral actions included in the control law and the SM is proposed. For CCAB, a SMC-based current tracking (SMCT) controller, including proportional, resonant and derivative control laws is presented. For both of the controllers, strict design process is followed, system stability in Lyapunov sense is guaranteed and convergence of the state errors to zero is strictly proved based on Barbalat' Lemma. Finally, comparative simulation studies on DPC under BVC and on CCAB are conducted to verify the effectiveness and to demonstrate superiority of the proposed controllers.

The paper is organized as follows. In section II, dynamic model of VSC for DPC in α - β RF is developed; the CSMC controller and the ISMC controller are designed. In section III, current dynamic model for CCAB is developed and the SMCT controller is designed. In section IV, simulation results are presented and section V concludes the paper.

II. ISMC-BASED DPC FOR VSC

Schematic of three-phase VSC is as shown in Fig.1. In the figure, e_a, e_b, e_c , and i_a, i_b, i_c represent grid voltage and current, respectively; v_a, v_b, v_c represent the converter pole voltage; L and R represent ac line inductance and resistance, V_{dc} and C represent dc bus voltage and dc bus capacitor, respectively. It's assumed that the grid voltage is three-phase balanced and the grid frequency is 50 Hz.

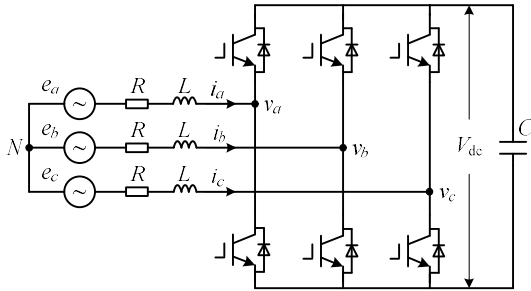


Fig. 1. Schematic of three-phase VSC.

A. Instantaneous Power Dynamic Model

Power dynamic model of VSC is developed in α - β RF. For DPC, the equivalent circuit is shown in Fig.2, where $E_{\alpha\beta}, V_{\alpha\beta}$ denote complex vectors of the grid voltage and converter pole voltage, and $I_{\alpha\beta}$ denotes complex vector of the grid current.

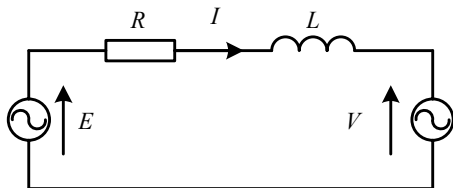


Fig. 2. Equivalent circuit of VSC for direct power control.

From Fig.1 and Fig.2, we can have:

$$\begin{cases} e_\alpha = L \frac{di_\alpha}{dt} + Ri_\alpha + v_\alpha \\ e_\beta = L \frac{di_\beta}{dt} + Ri_\beta + v_\beta \end{cases} \quad (1)$$

where $e_\alpha, e_\beta, i_\alpha$, and i_β are the α - and β -axis grid voltage and current components, and v_α, v_β the α - and β -axis converter pole voltage components.

Define:

$$\begin{cases} e_\alpha = E_m \cos(\omega t + \theta_e), e_\beta = E_m \sin(\omega t + \theta_e) \\ i_\alpha = I_m \cos(\omega t + \theta_i), i_\beta = I_m \sin(\omega t + \theta_i) \end{cases} \quad (2)$$

where E_m, I_m are amplitudes and θ_e, θ_i the initial phases of grid voltage and current, respectively.

The instantaneous active power (P) and reactive power (Q) at the point of common coupling (PCC) are:

$$P + jQ = \frac{3}{2} E_{\alpha\beta} \times I_{\alpha\beta}^* \quad (3)$$

with:

$$\begin{cases} E_{\alpha\beta} = E_\alpha + jE_\beta \\ I_{\alpha\beta} = I_\alpha + jI_\beta \end{cases} \quad (4)$$

and $I_{\alpha\beta}^*$ is the complex conjugate of $I_{\alpha\beta}$.

Substituting (4) into (3) and through some mathematical manipulations, P and Q can be calculated as:

$$\begin{bmatrix} P \\ Q \end{bmatrix} = \frac{3}{2} \begin{bmatrix} e_\alpha & e_\beta \\ e_\beta & -e_\alpha \end{bmatrix} \begin{bmatrix} i_\alpha \\ i_\beta \end{bmatrix} \quad (5)$$

Variations of P and Q can be calculated from (5) as:

$$\begin{cases} \frac{dP}{dt} = \frac{3}{2} \left(e_\alpha \frac{di_\alpha}{dt} + i_\alpha \frac{de_\alpha}{dt} + e_\beta \frac{di_\beta}{dt} + i_\beta \frac{de_\beta}{dt} \right) \\ \frac{dQ}{dt} = \frac{3}{2} \left(e_\beta \frac{di_\alpha}{dt} + i_\alpha \frac{de_\beta}{dt} - e_\alpha \frac{di_\beta}{dt} - i_\beta \frac{de_\alpha}{dt} \right) \end{cases} \quad (6)$$

According to (2), instantaneous variations of grid voltage can be expressed as:

$$\begin{cases} \frac{de_\alpha}{dt} = -\omega E_m \sin(\omega t + \theta_e) = -\omega e_\beta \\ \frac{de_\beta}{dt} = \omega E_m \cos(\omega t + \theta_e) = \omega e_\alpha \end{cases} \quad (7)$$

According to (1), instantaneous variations of grid current can be obtained as:

$$\begin{cases} \frac{di_\alpha}{dt} = \frac{1}{L} (e_\alpha - Ri_\alpha - v_\alpha) \\ \frac{di_\beta}{dt} = \frac{1}{L} (e_\beta - Ri_\beta - v_\beta) \end{cases} \quad (8)$$

Substituting (7) and (8) into (6), and through some mathematical manipulations, we have:

$$\begin{cases} \frac{dP}{dt} = \frac{3}{2L} [(e_\alpha^2 + e_\beta^2) - (e_\alpha v_\alpha + e_\beta v_\beta)] - \frac{R}{L} P - \omega Q \\ \frac{dQ}{dt} = \frac{3}{2L} (-e_\beta v_\alpha + e_\alpha v_\beta) - \frac{R}{L} Q + \omega P \end{cases} \quad (9)$$

B. The CSMC Controller

Denote $P_e = P - P_r, Q_e = Q - Q_r$ the active and reactive power errors, and P_r, Q_r the respective power references. Taking P_e and Q_e as new state variables, (9) can be expressed as:

$$\begin{cases} \frac{dP_e}{dt} = \frac{3}{2L} [(e_\alpha^2 + e_\beta^2) - (e_\alpha v_\alpha + e_\beta v_\beta)] - \frac{R}{L} P - \omega Q \\ \frac{dQ_e}{dt} = \frac{3}{2L} (-e_\beta v_\alpha + e_\alpha v_\beta) - \frac{R}{L} Q + \omega P \end{cases} \quad (10)$$

Define:

$$x = [P_c \quad Q_c]^T$$

Considering parameter uncertainty and disturbances in the system, (10) can be expressed in a compact form as:

$$\dot{x} = F_1(x) + G_1(x)u_0 + \delta_1(t, x) \quad (11)$$

where $u_0 = [v_{0\alpha} \ v_{0\beta}]^T$ denotes the control input, $G_1(x)$ denotes the control gain matrix, $F_1(x) = [F_{1P}(x) \ F_{1Q}(x)]^T$ denotes the nonlinear functions in the dynamic equations, $\delta_1(t, x)$ denotes the lumped uncertainty introduced by parameter uncertainty and external disturbances, with:

$$\begin{cases} F_{1P}(x) = \frac{3}{2L}(e_\alpha^2 + e_\beta^2) - \frac{R}{L}P - \omega Q \\ F_{1Q}(x) = \frac{R}{L}Q - \omega P \end{cases} \quad (12)$$

$$G_1(x) = \frac{-3}{2L} \begin{bmatrix} e_\alpha & e_\beta \\ e_\beta & -e_\alpha \end{bmatrix} \quad (13)$$

$$\delta_1(t, x) = [\delta_{1P}(t, x) \ \delta_{1Q}(t, x)]^T \quad (14)$$

Assume $\delta_1(t, x)$ satisfies:

$$|\delta_1(t, x)| \leq \rho_1(x)$$

where $\rho_1(x) = [\rho_{1P}(x) \ \rho_{1Q}(x)]^T$ with:

$$|\rho_{1P}(x)| \leq \rho_{1PM}, \quad |\rho_{1Q}(x)| \leq \rho_{1QM}.$$

In the following, arguments of various functions will not be written for the sake of convenience.

Define the SM as:

$$S_0 = [S_{0P} \ S_{0Q}]^T = [P_c \ Q_c]^T \quad (15)$$

Utilizing $U_0 = 0.5S_0^T S_0$ as the Lyapunov function candidate, then, derivative of U_0 along system state trajectories can be obtained as:

$$\dot{U}_0 = S_0^T \dot{S}_0 = S_0^T (F_1 + G_1 u_0 + \delta_1) \quad (16)$$

If the control law is designed as:

$$u_0 = -G_1^{-1}(F_1 + K_1 S_0 + v_0) \quad (17)$$

where:

$$K_1 = \text{diag}(K_{1P}, K_{1Q})$$

with $K_{1P}, K_{1Q} > 0$, and $\text{diag}(a_1, a_2)$ denotes a diagonal matrix with a_1 and a_2 as the main diagonal elements, and:

$$v_0 = \eta_0 \text{sign}(S_0) = \text{diag}(\eta_{0P}, \eta_{0Q}) [\text{sign}(S_{0P}) \ \text{sign}(S_{0Q})]^T \quad (18)$$

for some $\eta_{0P} > \rho_{1PM}, \eta_{0Q} > \rho_{1QM}$.

Then, we have:

$$\dot{U}_0 = -S_0^T K_1 S_0 - (\eta_{0P} - \rho_{1PM}) |S_{0P}| - (\eta_{0Q} - \rho_{1QM}) |S_{0Q}| \leq 0.$$

According to Barbalat's lemma, we can conclude S_{0P}, S_{0Q} asymptotically converge to the equilibrium point.

To reduce the chattering, the signum function in (17) is often replaced with a high-slope saturation function as:

$$\text{sat}\left(\frac{S_{0m}}{\varepsilon_{0m}}\right) = \begin{cases} 1, & \text{if } S_{0m} > \varepsilon_{0m} \\ S_{0m}/\varepsilon_{0m}, & \text{if } |S_{0m}| \leq \varepsilon_{0m} \\ -1, & \text{if } S_{0m} < -\varepsilon_{0m} \end{cases} \quad (19)$$

where subscript $m = P, Q$, and $\varepsilon_{0m} > 0$ denotes width of the boundary layer.

Block diagram of the CSMC controller is as shown in Fig.3. We can see from the figure the CSMC controller is in essence a SMC-based proportional controller. This means that it alone

cannot provide accurate power control when time delays in the control loop are non-negligible. For rectifier and inverter operation mode, structures of the control system are different; working principles of the CSMC controller for these two modes are described as follows.

When the VSC is operated in the rectifier mode, the active power control loop is cascaded with the dc voltage control loop. For active power control, the following power balance relationship holds.

$$P_{ac} = P_{dc} = V_{dc}^2 / R_L \quad (20)$$

where P_{ac} is the active power supplied by the ac system and P_{dc} is the power consumed in the dc system, including the loss consumed in the circuits. Therefore, if V_{dc} is controlled at the nominal value through PI controller, P equals the actual active power demand. For reactive power control, there's only the control force provided by the CSMC controller. Under this circumstance, the steady state power errors cannot be fully eliminated, especially for high power VSC-based applications. Moreover, to reduce the errors, high proportional gains have to be adopted, which poses potential threats on performance as well as stability of the system.

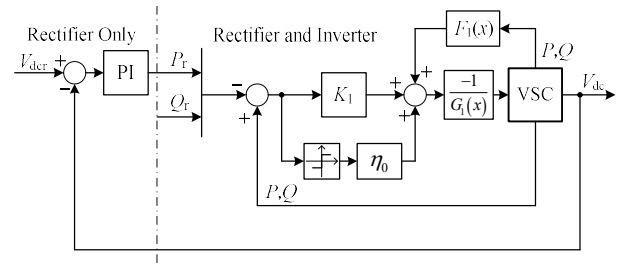


Fig. 3. Block diagram of the CSMC controller.

When operated as grid-connected inverters, structure of the control system for VSC is symmetric. There's only the control force provided by the CSMC controller. As a consequence, non-zero steady state errors will be produced for both active and reactive power control sub-systems.

C. The ISMC Controller

To eliminate steady state power errors, integral actions are necessary. To this purpose, define:

$$x_0 = \left[\int P_c \quad \int Q_c \right]^T, \quad x_1 = [P_c \quad Q_c]^T.$$

Express (11) and the x_0 dynamic in a compact form as:

$$\begin{cases} \dot{x}_0 = x_1 \\ \dot{x}_1 = F_1(x) + G_1(x)u_1 + \delta_1(t, x) \end{cases} \quad (21)$$

Define the integral SM as:

$$S_1 = \begin{bmatrix} S_{1P} \\ S_{1Q} \end{bmatrix} = \begin{bmatrix} P_c \\ Q_c \end{bmatrix} + K_1 \begin{bmatrix} \int P_c \\ \int Q_c \end{bmatrix} \quad (22)$$

Utilizing $U_1 = 0.5S_1^T S_1$ as the Lyapunov function candidate, then, derivative of U_1 along system state trajectories can be obtained as:

$$\dot{U}_1 = S_1^T \dot{S}_1 = S_1^T (F_1 + K_1 x_1 + G_1 u_1 + \delta_1) \quad (23)$$

If the control law is designed as:

$$u_1 = -G_1^{-1}(F_1 + K_1 x_1 + K_{IS} S_1 + v_1) \quad (24)$$

where:

$$K_{IS} = \text{diag}(K_{ISP}, K_{ISQ})$$

for some $K_{1SP}, K_{1SQ} > 0$, and v_1 is:

$$v_1 = \eta_1 \text{sign}(S_1) = \text{diag}(\eta_{1P}, \eta_{1Q}) \left[\text{sign}(S_{1P}) \quad \text{sign}(S_{1Q}) \right]^T \quad (25)$$

with $\eta_{1P} > \rho_{1PM}, \eta_{1Q} > \rho_{1QM}$.

Then, we have:

$$\dot{U}_1 = -S_1^T K_{1S} S_1 - (\eta_{1P} - \rho_{1PM}) |S_{1P}| - (\eta_{1Q} - \rho_{1QM}) |S_{1Q}| \leq 0$$

Therefore, the system is asymptotically stable according to Barbalat's lemma. Then, $x_1 \rightarrow 0$ can be proved from definition of the sliding manifold S_1 in (22).

In (24), there's no need to replace the signum function with high slope saturation functions. This is because the integral of the active and reactive power errors and thereby the SMs are not zero under steady state, thus the chattering problem faced by the CSMC controller is solved naturally.

One thing to note is that if the control law u_1 is designed as:

$$u_1 = -G_1^{-1} (F_1 + K_{1x} x + v_1) \quad (26)$$

which is adopted in [13-15], we will get:

$$\dot{U}_1 = -(\eta_{1P} - \rho_{1PM}) |S_{1P}| - (\eta_{1Q} - \rho_{1QM}) |S_{1Q}| \leq 0$$

However, integral actions are included in the switching function only, which makes it equivalent to a proportional controller from control force's point of view. Consequently, steady state errors cannot be fully eliminated.

III. SMC-BASED CURRENT TRACKING CONTROL

A. Current Dynamic Model

Denote $i_{\alpha e} = i_{\alpha} - i_{\alpha r}$ and $i_{\beta e} = i_{\beta} - i_{\beta r}$ the α - and β -axis current errors and $i_{\alpha r}$ and $i_{\beta r}$ the respective references. Taking current errors as the new state variables, Eq. (2) can be expressed as:

$$\frac{dy}{dt} = F_2(y) + G_2(y)u_2 + \delta_2(y, u_2) \quad (27)$$

where $y = [i_{\alpha e} \quad i_{\beta e}]^T$ denotes the state variable, $u_2 = [v_{2\alpha} \quad v_{2\beta}]^T$ denotes the control input, $F_2(y) = [F_{2\alpha}(y) \quad F_{2\beta}(y)]^T$ denotes the nonlinear functions in dynamic equations, $G_2(y)$ denotes the control gain matrix, $\delta_2(y, u_2) = [\delta_{2\alpha}(y, u_2) \quad \delta_{2\beta}(y, u_2)]^T$ denotes the lumped uncertainty introduced by parameter uncertainty and external disturbances, with:

$$\begin{cases} F_{2\alpha}(y) = \frac{1}{L}(e_{\alpha} - Ri_{\alpha}) - di_{\alpha r} \\ F_{2\beta}(y) = \frac{1}{L}(e_{\beta} - Ri_{\beta}) - di_{\beta r} \end{cases} \quad (28)$$

$$G_2(y) = -\text{diag}(1, 1)/L \quad (29)$$

$$di_{\alpha r} = -\omega i_{\beta r}, di_{\beta r} = \omega i_{\alpha r} \quad (30)$$

Assume $\delta_2(y, u_2)$ satisfies:

$$|\delta_{2\alpha}(y, u_2)| \leq \rho_{2\alpha M}, |\delta_{2\beta}(y, u_2)| \leq \rho_{2\beta M}$$

for some positive real numbers $\rho_{2\alpha M}$ and $\rho_{2\beta M}$.

B. The SMCT Controller

The sliding manifolds for the α - and β -axis current control sub-systems are defined as:

$$S_2 = \begin{bmatrix} S_{2\alpha} \\ S_{2\beta} \end{bmatrix} = \begin{bmatrix} i_{\alpha e} \\ i_{\beta e} \end{bmatrix} + K_R GI \begin{bmatrix} i_{\alpha e} \\ i_{\beta e} \end{bmatrix} \quad (31)$$

where:

$$K_R = \text{diag}(K_{R\alpha}, K_{R\beta}),$$

$$GI = \text{diag}\left(\frac{2\omega_c s}{s^2 + 2\omega_c s + \omega^2}, \frac{2\omega_c s}{s^2 + 2\omega_c s + \omega^2}\right)$$

for some $K_{R\alpha}, K_{R\beta} > 0$.

In (31), ω_c is the bandwidth parameter of the generalized ac integrator (GI), and it determines the effective bandwidth of the GI. Here, we use the non-ideal GI instead of the ideal one to make it adapts to frequency variations.

Then, derivative of S_2 can be calculated as:

$$\dot{S}_2 = F_2 + G_2 u_2 + \delta_2 + K_R DGI(y) \quad (32)$$

with:

$$DGI = \text{diag}\left(\frac{2\omega_c s^2}{s^2 + 2\omega_c s + \omega^2}, \frac{2\omega_c s^2}{s^2 + 2\omega_c s + \omega^2}\right)$$

Utilizing $U_2 = 0.5S_2^T S_2$ as the Lyapunov function candidate, then, derivative of U_2 along system state trajectories can be obtained as:

$$\dot{U}_2 = S_2^T \dot{S}_2 = S_2^T [F_2 + G_2 u_2 + K_R DGI(y) + \delta_2] \quad (33)$$

If the control law is designed as:

$$u_2 = -G_2^{-1} [F_2 + K_R DGI(y) + K_{2S} S_2 + v_2] \quad (34)$$

where v_2 is:

$$v_2 = \eta_2 \text{sign}(S_2) = \text{diag}(\eta_{2\alpha}, \eta_{2\beta}) \left[\text{sign}(S_{2\alpha}) \quad \text{sign}(S_{2\beta}) \right]^T \quad (35)$$

and:

$$K_{2S} = \text{diag}(K_{2S\alpha}, K_{2S\beta})$$

for some $\eta_{2\alpha} > \rho_{2\alpha M}, \eta_{2\beta} > \rho_{2\beta M}$, and $K_{2S\alpha}, K_{2S\beta} > 0$.

Then, we have:

$$\dot{U}_2 \leq -S_2^T K_{2S} S_2 - (\eta_{2\alpha} - \rho_{2\alpha M}) |S_{2\alpha}| - (\eta_{2\beta} - \rho_{2\beta M}) |S_{2\beta}| \leq 0$$

Therefore, the system is asymptotically stable according to Barbalat's lemma. Then, $y \rightarrow 0$ can be proved from definition of the sliding manifold S_2 in (31).

IV. SIMULATION STUDIES AND RESULTS

A. General Configuration

Main parameters of the VSC studied are listed in Table I. The switching frequency is 2.0 kHz, and the control period is 100 μ s. Considering time delays exist in the control loops, a delay of 100 μ s is inserted between the modulation reference output and the space vector pulse width modulation generator. Besides, a dead time of 2 μ s is set for the gate on signals of each switching device.

TABLE I
ELECTRICAL PARAMETERS OF THE VSC STUDIED

Parameters	Values	Parameters	Values
AC input voltage	660 V _{L-L}	Rated power	500 kW
Nominal dc voltage	1500 V	AC inductance	1.8 mH
AC resistance	12 m Ω	DC capacitance	30 mF

In the simulation, main parameters of the controllers used are as listed in Table II.

TABLE II
MAIN PARAMETERS OF THE PROPOSED CONTROLLERS

Parameters	Values	Parameters	Values
K_{1P}, K_{1Q}	50, 50	K_{1SP}, K_{1SQ}	1500, 1500
K_{2SP}, K_{2SQ}	1200, 1200	K_{RP}, K_{RQ}	30, 30

In the simulation results, per-unit values are used. The base

voltages are 540 V for ac system and 1500 V for dc system, the base power is 500 kVA. In the results, the subscripts “rec” and “inv” denotes the rectifier and inverter operation modes respectively, and the subscripts “r” denotes the references of respective variables.

B. Simulation Results

In Fig.4 and Fig.5, performance of the ISMC controller is compared with the CSMC controller.

In Fig.4 (a) and (b), responses of VSC operated as rectifier to active and reactive power step changes by the CSMC and ISMC controllers are shown respectively. As ac voltage and current are symmetric, only the voltage and current of phase A are shown.

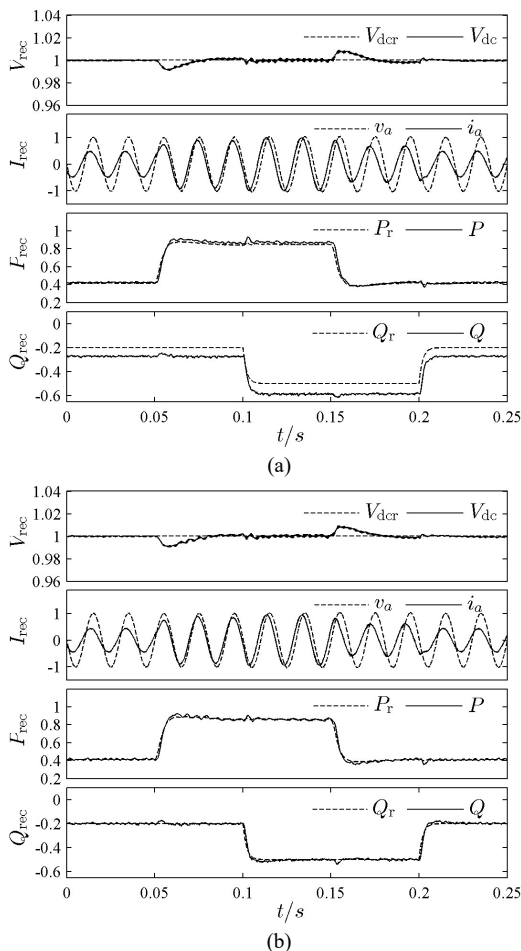


Fig. 4. Responses of the VSC operated as rectifier to power step changes for DC bus voltage (V_{dc}), phase A current (i_a), active power (P), reactive power (Q), by the (a) CSMC controller and the (b) ISMC controller.

From Fig.4 (a) we can see that active power, and thus the dc bus voltage is controlled accurately, owing to integral actions provided by the outer dc bus voltage (PI) controller. However, there're obvious steady state errors in the reactive power, due to lack of integral actions.

We can see from Fig.4 (b) that system responses by the ISMC controllers are satisfactory in terms of both transient and steady state performance. The response speeds of active and reactive power control sub-systems to power step changes are fast, the steady state power errors are fully eliminated.

In Fig.5, responses of VSC operated as inverter to power step changes are shown. As dc bus voltage is not controlled in this operation mode, it's not shown here.

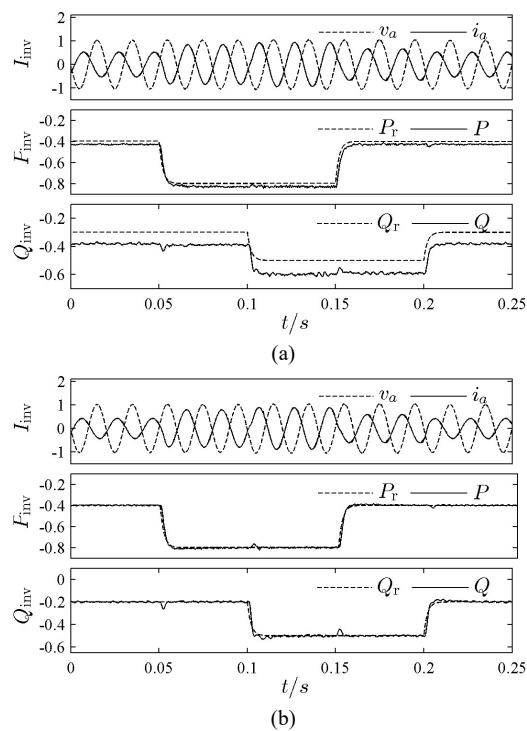


Fig. 5. Responses of the VSC operated as inverter to power step changes for phase A current (i_a), active power (P), reactive power (Q), by the (a) CSMC controller and the (b) ISMC controller.

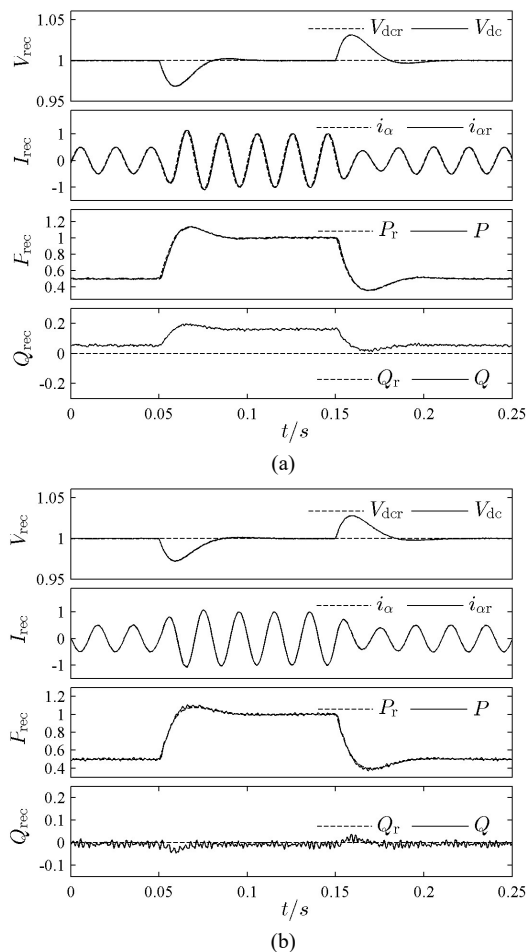


Fig. 6. Responses of the VSC operated as rectifier to power step changes for DC bus voltage (V_{dc}), ac current (i_a), active power (P), reactive power (Q), by the (a) PR controller and the (b) SMCT controller.

From Fig.5 (a) and (b) we can see that there're steady state errors in both the active and reactive power outputs by the

CSMC controller, and satisfactory transient and steady state performance are obtained by the ISMC controller.

In Fig.6 and Fig.7, performance of the SMCT controller is compared with the PR controller. To show current tracking performance of these controllers, the α -axis ac current and its reference are shown.

In Fig.6 (a) and (b), responses of VSC operated as rectifier to active and reactive power step changes by the PR and SMCT controllers are shown respectively.

From Fig.6 (a) we can see there're steady state errors in the reactive power outputs by the PR controller. The active power can be accurately controlled due to the outer dc voltage (PI) control loop. From Fig.6 (b) we can see satisfactory transient and steady state performance are obtained by the proposed SMCT controller. Fast response speeds and low overshoots are obtained, and both active and reactive power terms are accurately controlled. We can also see that there're current tracking errors for the PR controller, and current outputs track accurately their references for the SMCT controller.

In Fig.7, responses of VSC operated as inverter to power step changes are shown. As dc link voltage is not controlled in this operation mode, it's not shown in the figures.

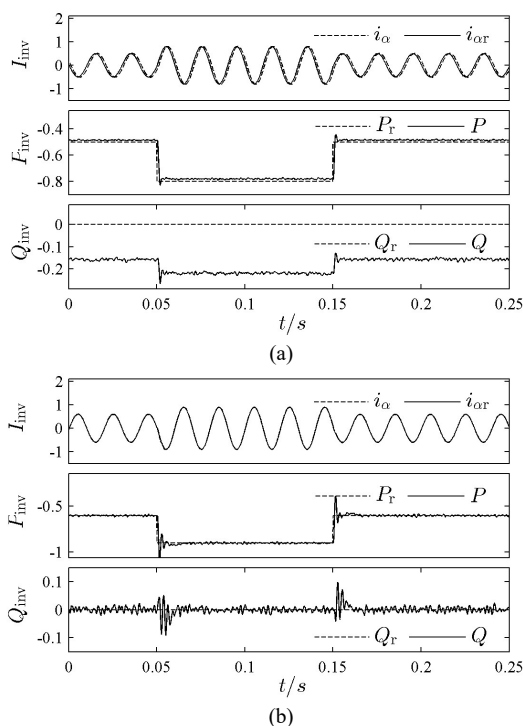


Fig. 7. Responses of the VSC operated as inverter to power step changes for ac current (i_α), active power (P), reactive power (Q), by the (a) PR controller and the (b) SMCT controller.

From Fig.7 (a) we can observe obvious steady state errors in the active and reactive power outputs by the PR controller, and there're also obvious current tracking errors. We can see from Fig.7 (b) that the current reference is accurately tracked and as a result, both the active and reactive power terms are accurately controlled.

V. CONCLUSIONS

This paper addresses practical SMC-based controllers for VSC. As time delays are inevitable in VSC-based systems, accurate current and power regulation cannot be obtained if

integral actions are not included, and current tracking errors will also be produced if PR controller is adopted. The CSMC controller is in essence a SMC-based proportional controller and thus steady state errors cannot be eliminated. The ISMC controller includes the integral actions, so that it's capable of eliminating fully the steady state errors. The SMCT controller includes proportional, resonant and derivative laws, which makes it an excellent tracking controller. Besides, derivatives of the current references are obtained by simple algebraic operations. This simplifies significantly the controller design. In designing the ISMC and the SMCT controllers, system stability in Lyapunov sense are guaranteed and convergence of the state errors to zero are proved based on Barbalat's Lemma. The theoretical analysis and simulation results are in good agreement, which verifies effectiveness and superiority of the proposed controllers.

REFERENCES

- [1] Dehkordi N M, Sadati N, and Hamzeh M, "A robust backstepping high-order sliding mode control strategy for grid-connected DG units with harmonic/ interharmonic current compensation capability," IEEE Transactions on Sustainable Energy, vol. 8, no. 2, pp. 561-572, 2017.
- [2] Obichere, J. K., M. Jovanovic, and S. Ademi, "Improved power factor controller for wind generator and applications," Engineering Letters, vol. 24, no.2, pp. 125-131, 2016.
- [3] Hao X, Yang X, Liu T, et al, "A sliding-mode controller with multiresonant sliding surface for single-phase grid-connected VSI with an LCL filter," IEEE Transactions on Power Electronics, vol. 28, no.5, pp. 2259-2268, 2013.
- [4] Yan S, Zhang A, Zhang H, et al, "Control scheme for DFIG converter system based on DC-transmission," IET Electric Power Applications, vol. 11, no. 8, pp.1441-1448, 2017.
- [5] Karaca H, and Bektas E, "Selective harmonic elimination using genetic algorithm for multilevel inverter with reduced number of power switches," Engineering Letters, vol. 24, no.2, pp.138-143, 2016.
- [6] Zhou G L, Shi X C, Wei X G, et al, "Sliding-mode control based VSC-HVDC under unbalanced input voltage condition," Proceedings of the CSEE, vol. 28, no. 22, pp. 137-143, 2008.
- [7] Yang W, Zhang A, Li J, et al, "Integral plus resonant sliding mode direct power control for VSC-HVDC systems under unbalanced grid voltage conditions," Energies 2017, 10(10), 1528, DOI: 10.3390/en10101528.
- [8] Moharana, A., and P. K. Dash, "Input-output linearization and robust sliding-mode controller for the VSC-HVDC transmission link," IEEE Transactions on Power Delivery, vol. 25, no. 3, pp. 1952-1961, 2010.
- [9] Shang, L., D. Sun, and J. Hu, "Sliding-mode-based direct power control of grid-connected voltage-sourced inverters under unbalanced network conditions," IET Power Electronics, vol. 4, no. 5, pp. 570-579, 2011.
- [10] Zhang, D., Wei, Y., Ma, L., et al, "Sliding mode control for grid-side converters of DFIG-based wind-power generation system under unbalanced grid voltage conditions," Transactions of China Electrotechnical Society, vol. 30, no. 10, pp. 266-275, 2015.
- [11] Shang L, and Hu J, "Sliding-mode-based direct power control of grid-connected wind-turbine-driven doubly fed induction generators under unbalanced grid voltage conditions," IEEE Transactions on Energy Conversion, vol. 27, no. 2, pp. 362-373, 2012.
- [12] Hu J, Shang L, and He Y, "Direct active and reactive power regulation of grid-connected DC/AC converters using sliding mode control approach," IEEE Transactions on Power Electronics, vol. 26, no. 1, pp. 210-222, 2011.
- [13] Sun D, Wang X, Nian H, et al, "A sliding-mode direct power control strategy for DFIG under both balanced and unbalanced grid conditions using extended active power," IEEE Transactions on Power Electronics, 2017, DOI: 10.1109/TPEL.2017.2686980.
- [14] Hu J, Nian H, Hu B, et al, "Direct active and reactive power regulation of DFIG using sliding-mode control approach," IEEE Transactions on Energy Conversion, vol. 25, no. 4, pp. 1028-1039, 2010.
- [15] Tan, Siew Chong, Y. M. Lai, et al, "Indirect sliding mode control of power converters via double integral sliding surface," IEEE Transactions on Power Electronics, vol. 23, no. 2, pp. 600-611, 2008.

- [16] Yang W, Zhang A, Zhang H, et al, "Adaptive integral sliding mode direct power control for VSC-MVDC system converter stations," International Transactions on Electrical Energy Systems, 2018, DOI: 10.1002/etep. 2516.
- [17] Gong H, Wand Y, Li Y, et al, "An input-output feedback linearized sliding mode control for D-STATCOM," Automation of Electric Power Systems, vol. 40, no. 5, pp. 102-108, 2016.
- [18] Sun L X, Chen Y, Wang Z, et al, "Optimal control strategy of voltage source converter-based high-voltage direct current under unbalanced grid voltage conditions," IET Generation Transmission & Distribution, vol. 10, no. 2, pp. 444-451, 2015.
- [19] Li S, Wang X, Yao Z, et al, "Circulating current suppressing strategy for MMC-HVDC based on nonideal proportional resonant controllers under unbalanced grid conditions," IEEE Transactions on Power Electronics, vol. 30, no. 1, pp. 387-397, 2015.
- [20] Wang Z, Zhang A, Zhang H, et al, "Control strategy for modular multilevel converters with redundant sub-modules using energy reallocation," IEEE Transactions on Power Delivery, vol. 32, no. 3, pp. 1556-1564, 2017.
- [21] Nian H, Shen Y, Song Y, "Direct power control strategy of grid connected inverter under unbalanced and harmonic grid voltage," Power System Technology, vol. 38, no. 6, pp. 1452-1458, 2014.

Weipeng Yang (M'17) received the B.S. degree in Automatic Control from Chang'an University, Xi'an China, and the M.S. degree in Electrical Engineering from Xi'an Jiaotong University, Xi'an China. He has been engaged in electric power system design from 2006 to 2014. He is now pursuing the Ph.D. degree in Electrical Engineering at Xi'an Jiaotong University. His research areas include dc distribution network, high power electronics converters, distributed generations and application of adaptive and robust control techniques.

Aimin Zhang received the B.S., M.S., and Ph.D. degrees all in Electrical Engineering from Xi'an Jiaotong University, Xi'an China. She has been with the School of electronic and information engineering, Xi'an Jiaotong University since 1984 and has been a professor there since 2012. Her research areas include adaptive and robust control theory and engineering, flexible ac transmission systems, and control of renewable generations.

Jungang Li received the B.S. degree in Mineral Processing from Central South University in 2004 and the M.S. degree in Electrical Engineering from Xi'an Jiaotong University in 2007. He is currently a senior engineer in the State Grid Xuji Group. His current research interests include substation automation, control and protection of distribution network, and hybrid AC/DC distribution network.

Jianhua Wang received the B.S., M.S. and Ph.D. degrees all in Electrical Engineering from Xi'an Jiaotong University in 1979, in 1983, and in 1985 respectively. He is currently a Professor in the School of Electrical Engineering, Xi'an Jiaotong University. His current research interests include intelligent apparatus technique, intelligent HV switchgear, and Micro-Grids.

Hang Zhang received the B.S. and M.S. degrees in Electrical Engineering from Xi'an Jiaotong University in 1983 and in 1985 respectively. He is currently an Assistant Professor in the School of Electrical Engineering, Xi'an Jiaotong University. His current research interests include HVDC transmission system and power electronics.